

MAS-NMR Studies of Carbonate Retention in a Very Wide Range of Na₂O-SiO₂ Glasses

BARROW, Nathan, PACKARD, Michael, VAISHNAV, Shuchi, WILDING, Martin, BINGHAM, Paul <<http://orcid.org/0000-0001-6017-0798>>, HANNON, Alex, APPLER, Matthew and FELLER, Steve

Available from Sheffield Hallam University Research Archive (SHURA) at:

<http://shura.shu.ac.uk/25762/>

This document is the author deposited version. You are advised to consult the publisher's version if you wish to cite from it.

Published version

BARROW, Nathan, PACKARD, Michael, VAISHNAV, Shuchi, WILDING, Martin, BINGHAM, Paul, HANNON, Alex, APPLER, Matthew and FELLER, Steve (2020). MAS-NMR Studies of Carbonate Retention in a Very Wide Range of Na₂O-SiO₂ Glasses. *Journal of Non-Crystalline Solids*, 534, p. 119958.

Copyright and re-use policy

See <http://shura.shu.ac.uk/information.html>

MAS-NMR Studies of Carbonate Retention in a Very Wide Range of Na₂O-SiO₂ Glasses

Nathan Barrow^a, Michael Packard^b, Shuchi Vaishnav^c, Martin C. Wilding^c, Paul A. Bingham^c, Alex C. Hannon^d, Matthew Appler^b and Steve Feller^b

^a *Johnson Matthey Technology Centre, Blount's Court, Sonning Common, Reading, RG4 9NH, UK*

^b *Physics Department, Coe College, Cedar Rapids, IA 52402, USA*

^c *Materials and Engineering Research Institute, Faculty of Science, Technology and Arts, Sheffield Hallam University, Sheffield, S1 1WB, UK*

^d *ISIS Facility, Rutherford Appleton Laboratory, Chilton, Didcot, Oxon, OX11 0QX, UK*

Abstract

Glasses that contain carbon are of geological interest, and the form of that carbon can be probed by Magic-Angle Spinning Nuclear Magnetic Resonance (MAS-NMR) spectroscopy. Previous studies of the Na₂O-SiO₂ glass system could only reach 56 mol% Na₂O. Here we reproduce and extend those studies to cover a very wide compositional range, from 20 to 70 mol% Na₂O, by using a combination of conventional melt-quench and twin roller quenching technologies on natural and 99% ¹³C-enriched sodium silicate glasses. ¹³C MAS-NMR reveals that measurable levels of carbon retention occur above at least 40 mol% Na₂O, and takes the form of CO₃²⁻ ions incorporated in the glass structure. These CO₃²⁻ anions are surrounded by Na⁺ cations, forming nanoscale domains in a sodium silicate glass network. ²³Na MAS-NMR showed a linear decrease in mean Na—O bond length with increasing Na₂O content, up to 60 mol% Na₂O, above which the mean Na—O bond length increased. Elemental analysis detected significant (>5%) carbonate by mass in the 65 and 70 mol% Na₂O glasses. For the 70 mol% Na₂O glass, ¹³C and ²³Na MAS-NMR detected ordered nanoscale domains composed of only Na₂O and CO₂. These results have shown the quantity and nature of carbon retention in the archetypal sodium silicate glass system, which will better inform structural models and carbonate solubility limits.

I. Introduction

Sodium silicate glass is the archetypical simple glass-forming system and is pivotal to our fundamental understanding of glass science. Sodium silicate forms the basis of many important glass applications such as flat glass, automobile glass, window glass, Pyrex and other borosilicates, bioglass, ion-strengthened glasses, and numerous industrial glasses¹⁻³. Yet for all its practical import the studied regime for these glasses is typically between 20 mol% and 50 mol% Na₂O. This is so because of phase separation and high liquidus temperatures and viscosities below 20 mol% Na₂O, and crystallization above 50 mol% Na₂O when the melt is cooled relatively slowly.

The conventional structural short-range model for the silicate network in the sodium silicate glass system is the *Lever-rule Model*⁴. The short-range structure is described by Q_n units where Q is a silicate tetrahedron and n is the number of bridging oxygens. The glasses proceed from Q₄ to Q₀ with a simplified binary model of Q_n transforming to Q_{n-1} as Na₂O content increases. Each Q unit has 4-n nearby sodium ions for charge balance. Thus, the charge of the Q_n tetrahedron is $-(4-n) = n-4$.

Previous studies have considered glasses containing up to 56 mol% Na₂O⁴. Through our access to twin-roller rapid quenching, for the first time we have been able to form and characterize Na₂O-SiO₂ glasses to 70 mol% Na₂O. We have performed the most comprehensive study of the structure and property of these glasses across the widest compositional range to date, namely 20 mol% to 70 mol% Na₂O by batch. These results are being reported in a series of linked papers, of which this is the first, covering a wide range of complementary techniques including neutron and X-ray diffraction, Raman and infrared spectroscopies, density, molar volume, atomic packing and thermal analysis, carbon elemental assay, and ¹³C, ²³Na and ²⁹Si MAS-NMR.

Here we focus on carbonate retention and structural aspects using a combination of carbon elemental assay and ¹³C / ²³Na high-field magic angle spinning nuclear magnetic resonance (MAS-NMR) studies. The ²⁹Si MAS-NMR results will be reported in a later paper and have been used to confirm and extend to new compositions beyond what has been reported for the structural evolution of the Q_n species. The diffraction data and the vibrational spectroscopy that will be presented in the linked papers will give supporting evidence for the Lever-rule model as well as the effects of carbonate retention on the structure. The various measures derived from density will be used to show how physical property data are influenced by short-range structure.

Substantial carbonate retention occurs in all alkali-containing oxide glass systems above a certain threshold alkali concentration^{5,6,7}. For example, for lithium borosilicate glass, RLi₂O.B₂O₃.KSiO₂, experiment and a model show that carbonate retention begins⁵ near an R value of 3 + 2K. For the sodium borate case the retention begins near⁶ R = 2 in RNa₂O.B₂O₃ and this causes glass formation to be enhanced above the orthoborate composition. The structural role of the carbonate has been unknown to date and is a thrust of the present paper.

II. Experimental Procedures

a. Sample preparation.

This investigation covers two sets of samples, one made with natural abundance Na_2CO_3 and one with 99% ^{13}C enriched Na_2CO_3 . The ^{13}C -enriched samples were also doped with a 0.1 wt% iron oxide (Fe_2O_3) to decrease the NMR relaxation time without affecting the peak widths or shifts⁸. Both sets of samples were synthesised under comparable conditions, and the melting process was identical for the corresponding samples from each set. Amorphous samples of nominal $x\text{Na}_2\text{O} \cdot (1-x)\text{SiO}_2$ compositions of $x = 0.20, 0.25, 0.30, 0.35, 0.40$ and 0.45 were produced by conventional melt quenching at Sheffield Hallam University, UK. The $x = 0.50$ glass crystallised upon cooling. A second attempt using splat quenching resulted in a partially amorphous sample. Glassy samples of composition $x = 0.45, 0.50, 0.55, 0.60, 0.65$, and 0.70 were made at Coe College, USA, using either plate quenching or a twin roller quencher, inside a dry nitrogen glove box. All of these samples had natural abundance carbon from sodium carbonate. Samples with ^{13}C enrichment were made at Coe College and had compositions of $x = 0.20, 0.25, 0.30, 0.35, 0.40, 0.45, 0.50, 0.55, 0.60, 0.65$, and 0.70 .

The starting materials at both Coe College and Sheffield Hallam University were Na_2CO_3 (natural abundance carbon) and SiO_2 of reagent grade ($>99.9\%$) or higher purity. 99% purity ^{13}C -enriched Na_2CO_3 was obtained from Cambridge Isotopes (Cambridge, Massachusetts, USA). Sodium carbonate was employed to provide a source of carbonate to be retained in the glasses. All reagents were well mixed and fused in platinum crucibles at temperatures ranging from 1140°C to 1550°C , with the higher temperatures necessary to melt the lower-sodium content glasses.

At Sheffield Hallam University batch compositions were prepared for 125g of glass using a calibrated balance with precision of ± 0.001 g, mixed thoroughly, and melted in a Pt-ZGS (ZrO_2 Grain Stabilized) crucible loosely covered with a Pt-ZGS lid to reduce Na_2O volatilization losses and contamination. The melts were attained within a temperature range of $1300\text{--}1470^\circ\text{C}$ (depending upon liquidus temperature and viscosity, as determined from appropriate phase diagrams and glass data), with a dwell time of 3 hours per melt, then poured onto a clean steel plate and allowed to cool gradually to room temperature. The glasses were not annealed. The cooled glasses were then immediately transferred into a vacuum desiccator to avoid hydration, in consideration of their limited chemical durability, particularly at lower SiO_2 contents. See Table 1 for additional details.

Samples made at Coe College were heated twice in pure platinum crucibles, and before the second heating a weight loss measurement was performed to check for carbonate retention. As above, the melt temperature range was $1140\text{--}1550^\circ\text{C}$ (depending upon liquidus temperature and viscosity as determined from appropriate phase diagrams and glass data), with a total heating time of approximately 25 minutes. Weight losses at high Na_2O contents that are below the predicted values, indicative of carbonate retention, were observed. Since clear, colorless, and bubble free samples were obtained in all cases, these melting times were found to be adequate.

Table 1 summarizes the preparation of the samples.

a. Natural C samples

Sample Source	$x\text{Na}_2\text{O}$ Composition (Mol. Fraction)	Heating Temperature ($^{\circ}\text{C}$)	Glass Weight (g)	Time (min)
Sheffield-Hallam	0.20	1470	125	180
Sheffield-Hallam	0.25	1430	125	180
Sheffield-Hallam	0.30	1380	125	180
Sheffield-Hallam	0.35	1350	125	180
Sheffield-Hallam	0.40	1330	125	180
Sheffield-Hallam	0.45	1300	125	180
Sheffield-Hallam	0.50	1260	125	180
Coe College	0.45	1200	6	25
Coe College	0.50	1200	6	25
Coe College	0.55	1200	6	25
Coe College	0.60	1200	6	25
Coe College	0.65	1140	6	25
Coe College	0.70	1140	6	25

b. ^{13}C enriched samples

Sample Source	$x\text{Na}_2\text{O}$ Composition (Mol. Fraction)	Fe_2O_3 content (g)	Heating Temperature ($^{\circ}\text{C}$)	Glass Weight (g)	Time (min)
Coe College	0.20	0.006	1550	6	25
Coe College	0.25	0.006	1450	6	25
Coe College	0.30	0.007	1450	6	25
Coe College	0.35	0.006	1350	6	25
Coe College	0.40	0.006	1350	6	25
Coe College	0.45	0.006	1200	6	25
Coe College	0.50	0.006	1200	6	25
Coe College	0.55	0.006	1200	6	25
Coe College	0.60	0.006	1200	6	25
Coe College	0.65	0.006	1140	6	25
Coe College	0.70	0.006	1140	6	25

Table 1. Formation details for the sodium silicate glasses

b. Carbon elemental assay

Carbon elemental assay was employed using a LECO CS844ES combustion furnace to measure the carbon content in the samples. The bulk glasses were crushed and milled at 700 rpm for a minute to produce glass powders. The powders were combusted in a high frequency induction furnace in the presence of pure O_2 gas until complete combustion was achieved. The analyses were carried out by an ISO 17025 (UKAS) accredited testing facility and the instrument was calibrated using appropriate Certified Reference Materials (CRMs). The range of calibrations covered all of the samples analyzed here, and additionally other CRMs were run as samples to confirm the calibration. These acted as independent validation of the calibration. Measurement uncertainties are provided as a percentage of the amount of carbon present in the sample, as

follows (% C in sample / % uncertainty of measured value): 3/2, 1/5, 0.2/5, <0.10/10, <0.005/20. The detection limit for these analyses was < 10 ppm (< 0.001%).

c. ^{13}C and ^{23}Na MAS-NMR experimental details

Solid-state MAS-NMR spectra were acquired at a static magnetic field strength of 14.1 T ($\nu_0(^1\text{H}) = 600$ MHz) on a Bruker Avance Neo console using TopSpin 4.0 software. A wide bore Bruker 4 mm MAS probe was used. For ^{13}C , the probe was tuned to 150.95 MHz and referenced to alanine CH_3 at 20.5 ppm. For ^{23}Na , the probe was tuned to 158.77 MHz and referenced to NaCl at 7.28 ppm. The glass pieces were ground by hand and packed into zirconia MAS rotors with Kel-F caps, in a dry nitrogen glovebox. Before and after weight measurements provided the sample mass for intensity normalization. Sodium carbonate was measured as received. The rotors were spun at 10 kHz for ^{13}C and 14 kHz for ^{23}Na , using room-temperature purified compressed air. Nutation tip angle was 90° for ^{13}C , and 45° for ^{23}Na . Relaxation times, unless otherwise stated, were 1000 s for ^{13}C and 0.01 s for ^{23}Na . To check for non-homogeneous distribution of Fe_2O_3 in the glass, saturation recovery experiments were performed. For the amorphous phase, there was no ^{23}Na line shape change between 0.01 s, 0.25 s and 10 s relaxation times. The locally ordered carbonate peaks continued to grow relative to the amorphous phase peak. Similarly, for the ^{13}C MAS-NMR, the more ordered carbonate had a much longer relaxation time than the amorphous phase. There was no indication of differential relaxation occurring in the ^{23}Na and ^{13}C spectra, which would manifest as a multi-exponential relaxation rate. For ^{13}C , between 4 and 32 scans were acquired using a one pulse acquisition program. For ^{23}Na , 8192 scans were acquired using a Hahn echo pulse sequence. ^{29}Si MAS-NMR details will be provided in a future paper in this series.

III. Results

a. Carbon elemental assay

Carbon retention in this glass system was quantified by LECO combustion furnace elemental analysis. At nominal compositions $x = 0.20, 0.25, 0.30$, and 0.35 Na_2O there was no more than 0.0001 weight fraction carbon detection. There was greater carbon retention with composition, and at the highest three compositions by Na_2O content, significant amounts of carbon were detected. At $x = 0.60$ Na_2O by batch the carbon detection was 0.0027 weight fraction, at $x = 0.65$ Na_2O the carbon detection was 0.0147 weight fraction, and at $x = 0.70$ Na_2O the carbon detection was 0.0305 weight fraction. To obtain the amount of carbon dioxide in the glasses we took the carbon assay results and converted to carbon dioxide concentration by

$$\begin{aligned} \text{Weight fraction } \text{CO}_2 &= w_{\text{C}} M_{\text{CO}_2} / M_{\text{C}} \\ &= 3.664 w_{\text{C}} \end{aligned} \quad (1)$$

where w_{C} is the detected weight fraction of carbon, and M_{CO_2} and M_{C} are the masses of CO_2 and C respectively. The weight fraction of CO_2 is plotted as a function of x in Figure 1. The onset of significant amounts of carbon dioxide retention is at approximately $x = 0.60$ Na_2O . It is noted that the samples containing 45 and 50 molar percent sodium oxide yielded closely similar

carbonate retention for samples prepared at Coe and Sheffield Hallam, consistent with the view that both sample preparation methods used in this paper yielded closely similar levels of carbonate retention in the final glasses, and consequently that CO₂ evolution during melting did not significantly differ between the two preparation approaches used.

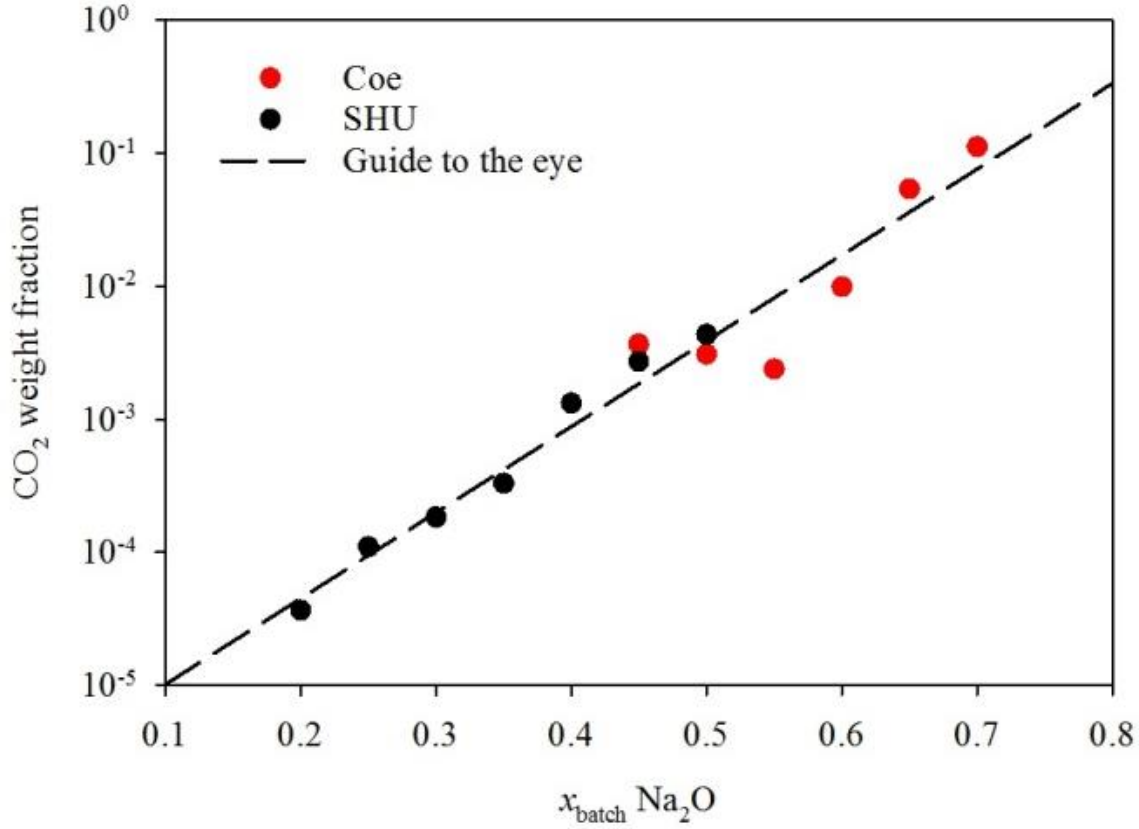


Figure 1. Weight fraction of CO₂ as a function of x on a semi-log plot. The dashed line is a guide to the eye.

Now that we have shown carbon is retained, we can correct the batch soda concentration to account for this retention. For this, we use the molar ratio J as a compositional parameter, where:

$$J = \frac{\text{Na}_2\text{O molar percent}}{\text{SiO}_2 \text{ molar percent}} \quad (2)$$

For a binary glass of composition $x\text{Na}_2\text{O} \cdot (1-x)\text{SiO}_2$, the molar ratio is:

$$J = \frac{x}{1-x} \quad (3)$$

The molar ratio, J_C , corrected for carbon retention (weight fraction w_C) was determined as follows: Consider a batch prepared with composition $J_{\text{batch}}(\text{Na}_2\text{CO}_3) \cdot \text{SiO}_2$. Upon heating carbon dioxide is released, and if there is no carbon retention then a glass of composition $J_{\text{batch}}\text{Na}_2\text{O} \cdot \text{SiO}_2$ is formed. However, a fraction f_C of the carbon atoms is retained (and two oxygen atoms are also retained for each carbon atom), with the result that the cooled glass actually has the following composition

$$J_{\text{batch}}(\text{Na}_2\text{O} \cdot f_C \text{CO}_2) \cdot \text{SiO}_2. \quad (4)$$

This formula can be re-written as follows

$$J_C(\text{Na}_2\text{O}) \cdot f_C J_{\text{batch}}(\text{Na}_2\text{CO}_3) \cdot \text{SiO}_2, \text{ where } J_C = J_{\text{batch}}(1 - f_C). \quad (5)$$

The LECO measurement provides the weight fraction of carbon in the glass, w_C , given by

$$w_C = \frac{f_C J_{\text{batch}} M_C}{J_{\text{batch}} M_{\text{Na}_2\text{O}} + f_C J_{\text{batch}} M_{\text{CO}_2} + M_{\text{SiO}_2}} \quad (6)$$

where M_C , M_{SiO_2} , $M_{\text{Na}_2\text{O}}$, and M_{CO_2} are the respective molecular masses. Re-arranging equation (6) gives

$$f_C = \frac{w_C (J_{\text{batch}} M_{\text{Na}_2\text{O}} + M_{\text{SiO}_2})}{J_{\text{batch}} (M_C - w_C M_{\text{CO}_2})} \quad (7)$$

Equation (7) allows us to use the LECO measurement of w_C to calculate the fraction of carbon that is retained. The resulting net modifications are shown in Table 2, as both corrected molar fractions of Na_2O and corrected J_C values. Figure 2 displays J_C vs J_{Batch} .

Batch $x\text{Na}_2\text{O}$ Content (Molar Fraction)	J_{Batch}	Weight Fraction Carbon w_C from LECO Analysis	Weight Fraction Carbon Dioxide from LECO Analysis	J_C	Corrected Molar Fraction (x) of Na_2O from LECO Analysis
0.70	2.333	0.0305	0.112	1.748	0.636
0.65	1.857	0.0147	0.054	1.631	0.620
0.60	1.500	0.0027	0.010	1.465	0.594
0.55	1.222	0.00065	0.002	1.215	0.549
0.50 (made at Coe)	1.000	0.00084	0.003	0.991	0.498
0.50 (made at SHU)	1.000	0.00118	0.004	0.988	0.497
0.45 (made at Coe)	0.818	0.00100	0.004	0.809	0.447
0.45 (made at SHU)	0.818	0.00074	0.003	0.811	0.448
0.40	0.667	0.00036	0.001	0.664	0.399
0.35	0.538	0.00009	0.000	0.538	0.350
0.30	0.429	0.00005	0.000	0.428	0.300
0.25	0.333	0.00003	0.000	0.331	0.250

0.20	0.250	0.00001	0.000	0.250	0.200
------	-------	---------	-------	-------	-------

Table 2: Effects of carbonate retention on compositions of sodium silicate glasses

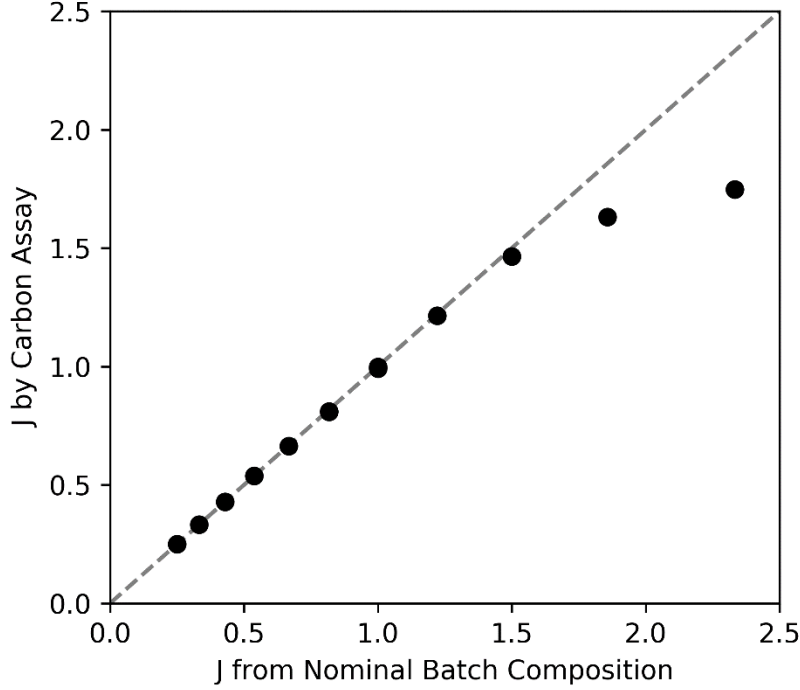


Figure 2: J_C , J corrected for carbon retention, as a function of J_{batch} .

The deviation between J_C and J_{batch} near $J = 1.5$ (60 mol% Na_2O) in Figure 2 is due to carbonate retention. To shed light on the nature of the retained carbon, we applied ^{13}C MAS-NMR.

b. Carbon and Sodium MAS-NMR

^{13}C MAS-NMR spectra from ^{13}C enriched samples are given in Figure 3 and clearly show the presence of carbon retention, in agreement with the elemental analysis results. From the chemical shift, we see that the carbon is present in the glasses in the form of CO_3^{2-} , rather than as dissolved CO_2 (or CO_2 gas trapped in bubbles).⁹ No carbon-silicon species were detected either, which would typically be expected to appear at approximately 20 ppm chemical shift¹⁰. In general, these NMR results show that more carbonate was retained for greater soda contents, consistent with the results of carbon elemental assay. Notably, ^{13}C MAS NMR was able to clearly detect the presence of carbonate even as low as $x = 0.40$. Up to 65 mol% Na_2O , the carbonate was all present in a locally disordered form as indicated by the presence of a broad (2 ppm FWHM) peak centered around 171.6 ppm.

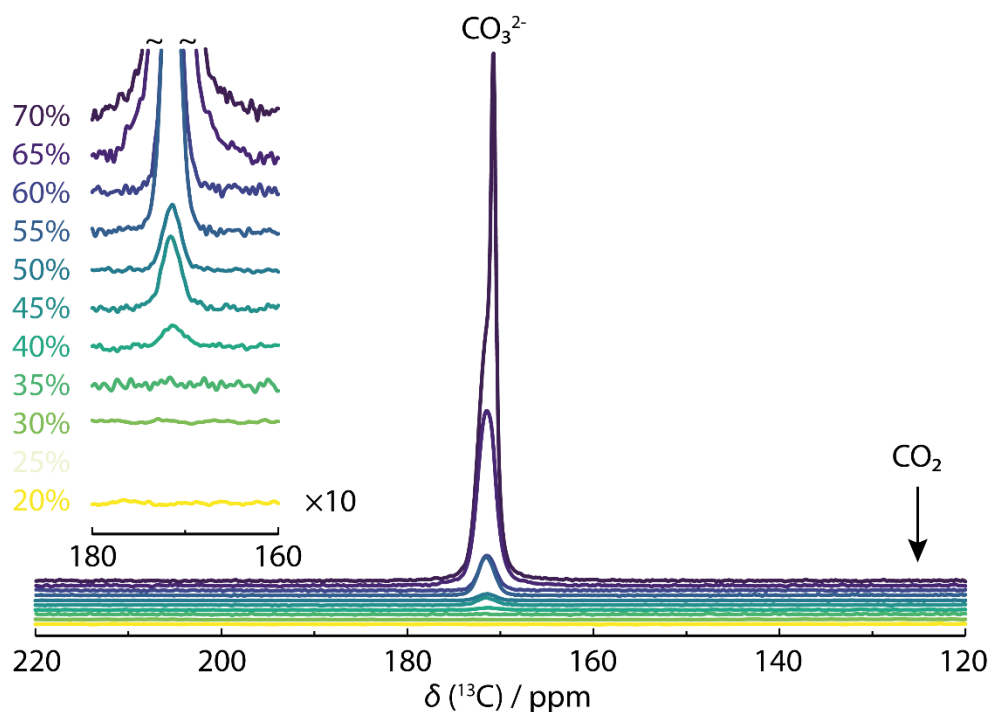


Figure 3. Normalized ^{13}C MAS-NMR spectra of $\text{Na}_2\text{O-SiO}_2$ glasses prepared using 99% ^{13}C -enriched Na_2CO_3 . Percentages indicate nominal glass composition in mol% Na_2O . Data for the 25 mol% Na_2O sample was not acquired for time efficiency as no signal was obtained for the 30 mol% Na_2O sample. The labels CO_3^{2-} and CO_2 represent locations for the chemical shift of those respective species.

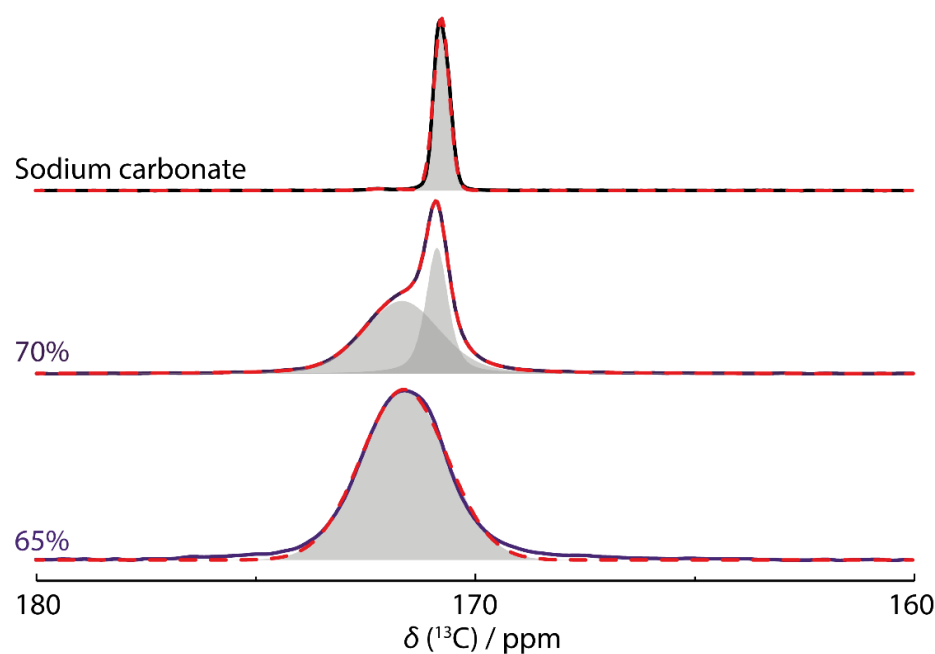


Figure 4. ^{13}C MAS NMR spectra of high soda $\text{Na}_2\text{O-SiO}_2$ glasses prepared using 99% ^{13}C -enriched Na_2CO_3 , along with a spectrum for pure crystalline Na_2CO_3 . Grey shapes are peak fits,

red dashed lines represent the sum of the fits. Spectra are not normalized, but scaled to the same height.

By analyzing the ^{13}C MAS-NMR spectra and comparing the $x = 0.70$ glass spectrum to the spectra for both crystalline Na_2CO_3 and $x = 0.65$ glass, two distinct carbonate environments are clearly observed, see Figure 4. Pure Na_2CO_3 presents one narrow peak, centered at 170.8 ppm, whereas the $x = 0.65$ glass presents a broad peak, centered at 171.6 ppm. However, the $x = 0.70$ glass presents both a narrow peak at 170.9 ppm and a broad peak at 171.5 ppm, see Figures 4 and 5. These chemical shifts and linewidths are consistent with previously measured crystalline sodium carbonate¹¹ and free sodium carbonate species⁹. This result implies that the $x = 0.70$ glass contains both locally-ordered and locally-disordered carbonate environments. The $\text{Na}_2\text{O-SiO}_2$ glasses in the range $x = 0.40$ to $x = 0.65$ only present the broad, locally-disordered carbonate environment, as shown in Figure 5.

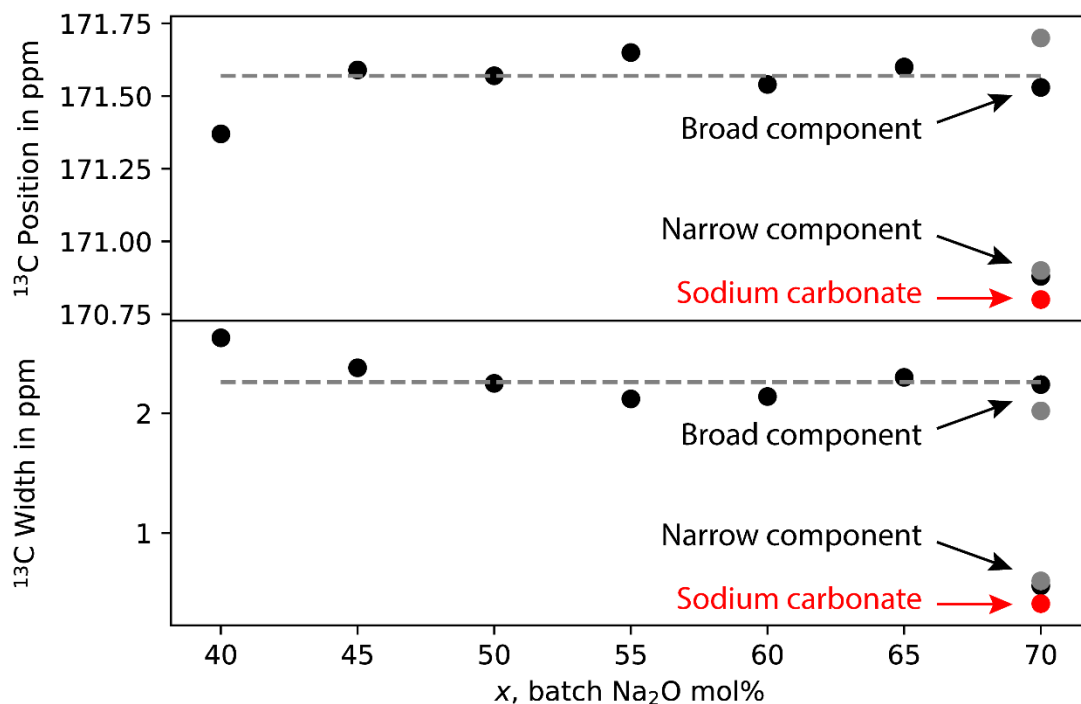


Figure 5. Fit parameters from ^{13}C MAS-NMR for $\text{Na}_2\text{O-SiO}_2$ glasses (black circles) and Na_2CO_3 (red circles, arbitrarily placed at 70 mol% Na_2O for comparison). Two data points for each component at 70 mol% Na_2O show the variation in fitting results if different Gaussian:Lorentzian (G/L) ratios are used. The black dots are the same as the other compositions where all peaks are fixed to be Gaussian. The grey dots present a best fit with G/L ratio of 0.74 (broad peak) and 0.48 (narrow peak). The dashed line is the mean of the broad fit parameters.

The normalized (by mass) ^{23}Na MAS-NMR spectra from $x = 20$ mol% to $x = 70$ mol% soda are shown in Figure 6. As expected, the ^{23}Na signal from the glasses intensifies with Na_2O content, simply because more sodium is present. The line shapes are broad, indicating all sodium is

present in a locally disordered form (note the fast relaxation time used). As the relatively high magnetic field of 14.1 T was used, the peak widths are predominately due to the distribution of chemical shifts, rather than second-order quadrupolar broadening¹¹.

Also observed is a systematic change in chemical shift to higher ppm (leftwards in Figure 6) as Na₂O content increases in the glasses. This is consistent with a shortening of the average Na—O bond length from approximately 2.80 Å to 2.56 Å¹²⁻¹⁴. For low-Na₂O glasses, and considering a Na⁺ ion, the probability is high that a neighboring O⁻ will be bonded to one or two Si⁴⁺. This Si—O covalent bond is stronger than the Na—O ionic bond, thus the oxygen will be much closer to silicon, especially where the oxygen is bridging two silicon atoms. For high-Na₂O glasses the probability is now much lower that neighboring O⁻ will be bonded to a silicon atom, rather the probability much higher that the neighboring O⁻ will be non-bridging and not-bonded to a silicon.

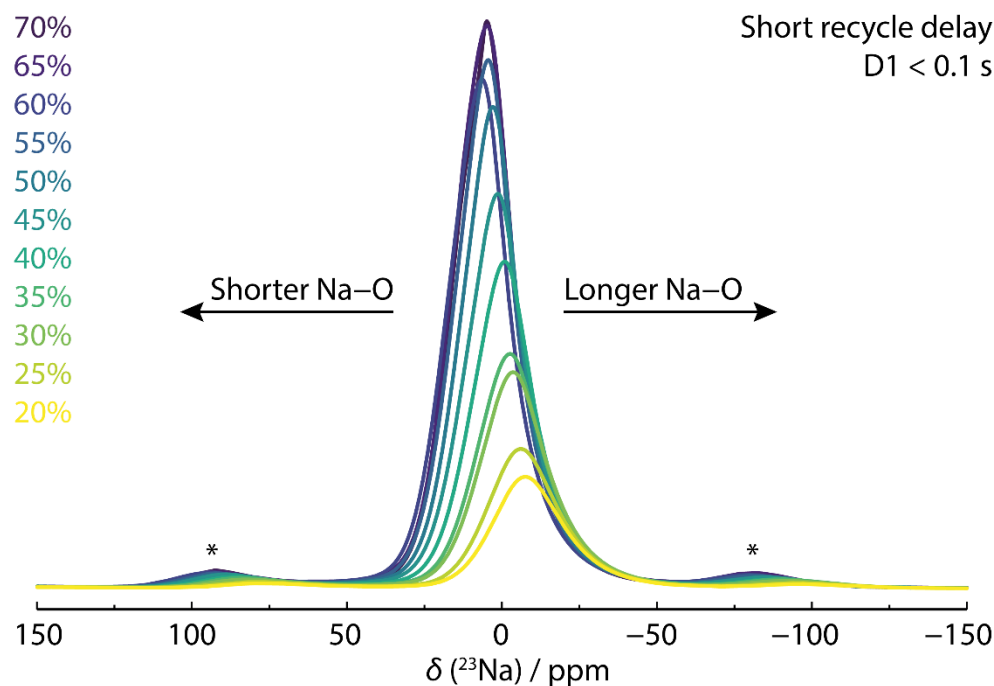


Figure 6. Normalized (by mass) ²³Na MAS NMR spectra at 14.1 T of sodium silicate glasses for 20 mol% to 70 mol% soda. Asterisks indicate spinning sidebands. Spectra acquired with a fast recycle delay.

Thus, as the coordination of sodium decreases a given Na⁺ ion will have a slightly stronger, and therefore shorter, bond with the O⁻. In NMR, when there are less electrons near the nucleus (e.g., a nearby oxygen atom is withdrawing them), this manifests as a chemical shift to higher ppm. Interestingly, as is often the case for amorphous materials, this change proceeds smoothly, at least for compositions between $x = 0.20$ to $x = 0.60$, see Figure 7. However, for compositions $x = 0.65$ and $x = 0.70$, the shift reverses. These very high Na₂O content glasses contain significant quantities of carbonate in their structure. As the carbon atom covalently bonds to its neighboring

oxygen atoms, they are pulled further away from the next-nearest neighboring Na^+ ions, hence the measured lengthening of the average Na—O bonds.

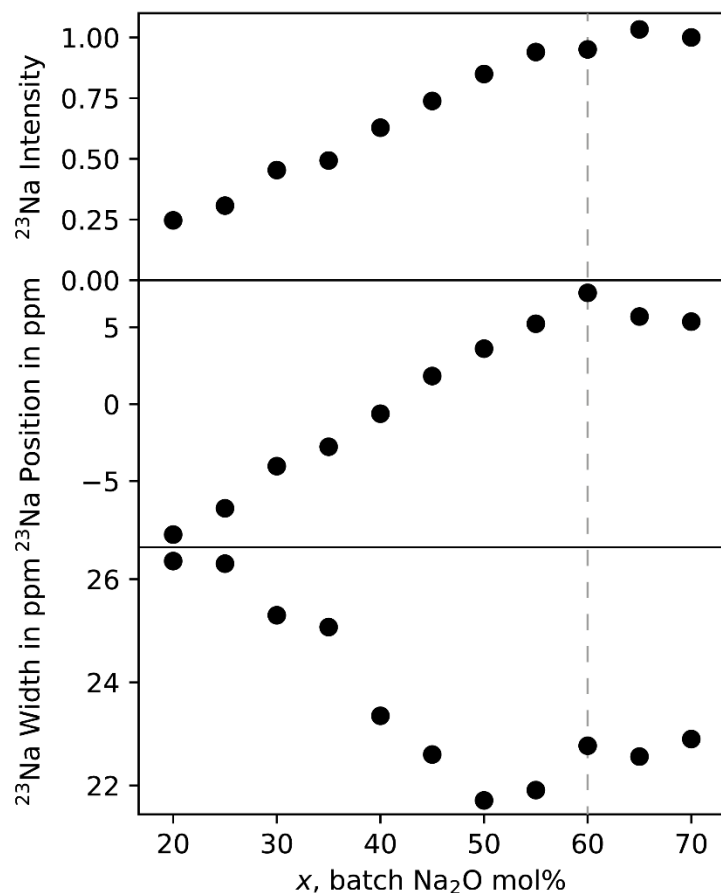


Figure 7. Selected fit parameters from ^{23}Na MAS-NMR for sodium silicate glasses obtained from DMFit¹⁵, with additional parameters given in Table 3. Pseudo-Voigt line shapes with chemical shift anisotropy were used as an approximate fit for each spectrum as a full fit would require modelling continuous distributions of both chemical shift and quadrupolar coupling. Intensity corresponds to normalized (by mass and number of scans) peak integral. Grey dashed line indicates $x = 0.60$, where the trend of peak position changes direction.

Batch $x\text{Na}_2\text{O}$ Composition (Mol. Fraction)	Amplitude	Position (ppm)	Width (ppm)	G/L ratio	CSA (ppm)	CSA eta	Integral [abs]
0.70	1.62E+09	5.37	22.90	0.64	-50.45	0.02	3.02E+14
0.65	1.57E+09	5.70	22.56	0.62	-45.67	0.89	3.12E+14

0.60	1.57E+09	7.24	22.77	0.57	-46.10	0.77	2.87E+14
0.55	1.5E+09	5.23	21.91	0.55	-44.33	0.66	2.84E+14
0.50	1.42E+09	3.61	21.71	0.55	-45.93	0.43	2.56E+14
0.45	1.12E+09	1.83	22.60	0.54	-51.40	0.55	2.23E+14
0.40	1.01E+09	-0.62	23.35	0.56	-51.61	0.38	1.9E+14
0.35	7.53E+08	-2.77	25.07	0.60	-56.46	0.84	1.49E+14
0.30	6.43E+08	-4.03	25.30	0.60	-53.41	0.84	1.37E+14
0.25	4.28E+08	-6.77	26.30	0.63	-59.64	0.74	9.27E+13
0.20	3.12E+08	-8.48	26.35	0.61	-56.28	0.88	7.44E+13

Table 3. ^{23}Na MAS-NMR fit parameters. G/L is the ratio of the Gaussian intensity to Lorentzian. CSA is chemical shift anisotropy

The spectra shown in Figure 6 were deliberately measured using a fast relaxation time (0.01 s) to view the locally disordered component of the glasses only. When a longer relaxation time is used (10 s), the spectra appear as shown in Figure 8. For compositions $x = 0.60$ and 0.65 the spectra are similar to the fast relaxation spectra, confirming that all of the sodium is present in the locally disordered phase. However, the spectrum for $x = 0.70$ shows two additional sharp peaks superimposed over the locally disordered peak, consistent with the presence of two different sodium-containing phases. These additional peaks can be assigned to Na_2CO_3 by comparison with the Na_2CO_3 reference spectrum also shown in Figure 8.

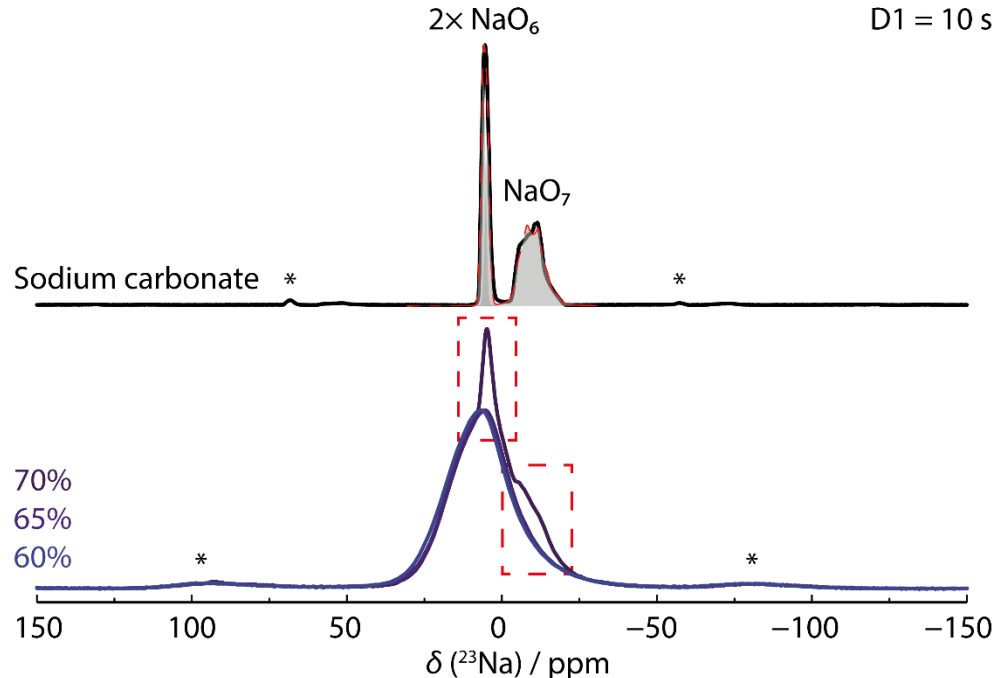


Figure 8. ^{23}Na MAS-NMR spectra of crystalline Na_2CO_3 and three high Na_2O content glasses. Asterisks indicate spinning sidebands. Spectra acquired with a slow recycle delay. Red dashed boxes indicate locally ordered sodium carbonate presence in the $x = 0.70$ glass. Deconvolutions of ^{23}Na Na signal from the sodium carbonate crystal are shown in grey. Spectra are not normalized, but scaled to the same height.

From the literature, we can assign the ^{23}Na peaks of sodium carbonate¹⁶⁻¹⁷. Two spherically symmetric octahedral sites share the leftmost peak (δ_{iso} between 5 ppm and 6.5 ppm), whereas the rightmost line shape ($\delta_{\text{iso}} = 3.4$ ppm) is from a third sodium ion neighboring to seven oxygen ions. This lack of spherical symmetry causes its peak shape to become broadened by the quadrupolar interaction ($C_Q = 2.4$ MHz, $\eta_Q = 0.5$). A deconvolved spectrum showing these three sites is given in Figure 8.

IV. Discussion

The results presented here greatly add to our knowledge of sodium silicate glasses. We have been able to detect carbonate retention, a ubiquitous effect in modified oxide glasses prepared using conventional raw materials, in the form of a useable ^{13}C symmetric MAS-NMR line shape, which indicates that the carbonate is locally disordered. We detected this signal even at $J = 0.67$ (40 molar percent Na_2O). According to the carbon assay results shown in Figure 1, the weight fraction of carbonate in this glass was just 0.001, i.e. 0.1 wt. %.

Understanding the factors and relationships governing the solubility of CO_2 in silicate melts, and the behavior of carbonate melts (some of which are also glass-forming) holds great interest across a wide range of fields¹⁸⁻²⁶. Geologists^{20-23,25,26} have carried out many studies of CO_2 in silicate glasses and melts, usually under high (GPa) applied pressures, and often in the presence of H_2O , in order to simulate deep geological conditions. Whilst our study here was not

specifically designed, or experimental conditions constrained, to provide CO₂ saturation of the melts, our results are nevertheless relevant. In particular, it has been shown that in some cases, carbon retention (as CO₂ or CO₃²⁻) in silicate melts yields linear relationships when plotted against the non-bridging oxygen per tetrahedron (NBO/T) ratio of the glass or melt²⁵. Plotting NBO/T (calculated as 2[Na₂O]/[SiO₂], neglecting the repolymerising effect of the CO₃ groups) vs. carbon content of our glasses, shows a very similar relationship to that shown in Figure 1 see Figure 9. This non-linear relationship is markedly different from those obtained, for example, by Brooker *et al.*²⁵ for multicomponent melts under high (GPa) applied pressures where a number of linear relationships were obtained. A linear approximation can, however, be obtained by plotting the logarithm of carbon content against NBO/T, this is shown in Figure 9.

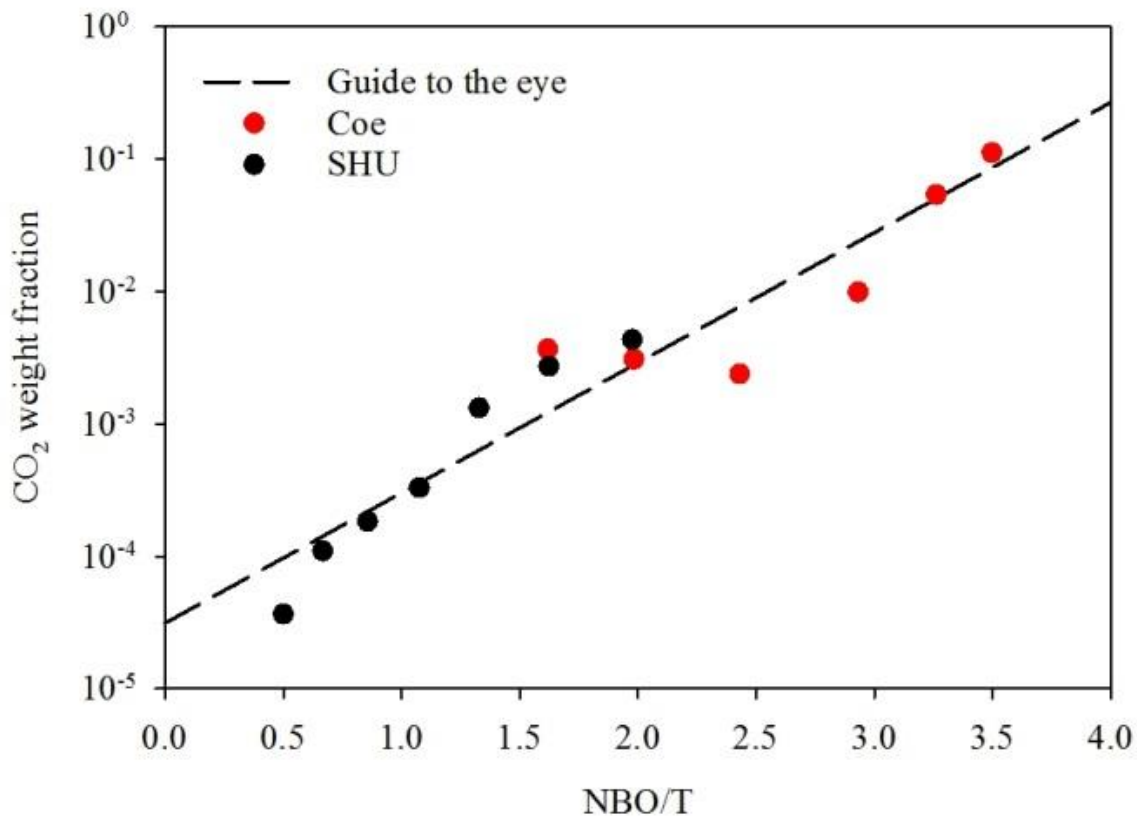


Figure 9: Carbon dioxide weight fraction as a function of fraction of non-bridging oxygen to tetrahedron ratio. The dashed line is a guide to the eye.

This behavior and its structural origins / relationships will be considered in detail in a forthcoming publication, however, it is worthwhile also briefly considering it here. The glasses studied here were prepared at atmospheric pressure, ~0.1 MPa or ~0.0001 GPa. Comparisons against data obtained for glasses prepared under pressure must be made carefully. Brooker *et al.*²⁵ showed an interesting relationship between CO₂ solubility and a very wide range of NBO/T (0 to 4), whereby at 2.0 GPa pressure an approximately linear relationship existed between CO₂ solubility and NBO/T, but at 0.2 GPa pressure this relationship has a sigmoid shape, whereby at lower NBO/T there is a lag in the increase of CO₂ solubility with NBO/T, and it does not begin

to increase significantly (when plotted on a linear scale) until NBO/T \sim 1. It is conceivable that such pressure-related behavior as highlighted by Brooker *et al.*²⁵ led to a similar but stronger sigmoid behavior for our samples (melted at 0.0001 GPa), whereby the CO₂ solubility does not begin to increase strongly until NBO/T = 2 to 3 (see Figure 1). This will be discussed further, in a structural context, in a forthcoming publication.

The ¹³C and ²³Na MAS-NMR results for glasses with nominal compositions between 20 and 65 mol% Na₂O show broad, featureless, mostly Gaussian peaks. This indicates that both carbon (in the form of free sodium carbonate species) and Na⁺ ions are present in locally disordered environments. This implies that the CO₃²⁻ ions are necessarily surrounded by Na⁺ ions, forming nanoscale domains within the sodium silicate glass network. These nanoscale domains are small enough (perhaps only a single carbonate unit) to have a range of bond lengths and angles, appearing amorphous in form. However, for the 70 mol% Na₂O sample, both ¹³C and ²³Na MAS-NMR reveal that some (< 30%) of the sodium is present in well-ordered Na₂CO₃ units. This abundance indicates that a larger domain size of Na₂CO₃ is present, distinct from the locally disordered sodium carbonate nanoscale domains. Supporting evidence comes from neutron scattering, the full details of which will be published in an associated paper. The neutron diffraction pattern of the sample with 70 mol% Na₂O shows some small Bragg peaks, arising from particles of crystalline γ -Na₂CO₃ of diameter \sim 100 Å, forming \sim 2% of the sample, see Figure 10.

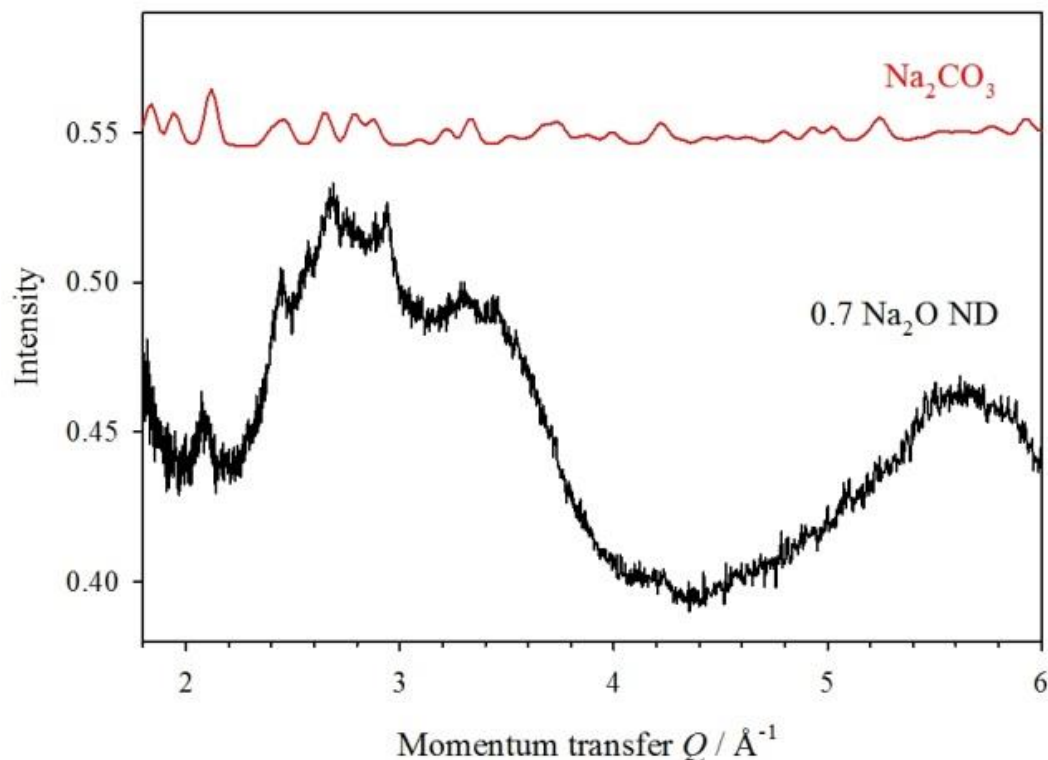


Figure 10. Neutron diffraction pattern for the 70 mol% Na₂O sample (black), together with a simulation for 100 Å crystallites of γ -Na₂CO₃, forming 2% of the sample.

Therefore, we propose that for smaller Na₂O contents the CO₃ groups occur as individual structural entities that are isolated from each other, but for 70 mol% Na₂O there is a significant number of CO₃ groups that occur in a cluster within the glass network, separated from each other only by Na⁺ ions, with a similar arrangement at the local scale to that in crystalline Na₂CO₃, but without the occurrence of long range order. Potentially, longer melting times may reduce or eliminate these inclusions²⁷, or perhaps between 65 and 70 mol% Na₂O represents the maximum solubility limit for CO₃²⁻ ions under the preparation conditions used here.

Comparison of our ¹³C MAS-NMR results with data for other sodium-bearing glasses yields further insight into the structure of our glasses and the local environments of carbon and sodium. Kohn *et al.*²⁸ and Brooker *et al.*²⁹ studied a series of sodium aluminosilicate and sodium-calcium aluminosilicate melts and glasses prepared under pressures of 1 to 2.5 GPa. Kohn *et al.*'s²⁸ NaAlSiO₄ glass gave an asymmetric peak centered at ~163 ppm with additional, weaker components towards lower chemical shifts, creating asymmetry in the overall band. Conversely, their soda-melilite (CaNaAlSi₂O₇) glass provided a single, symmetrical peak centered at ~168 ppm. For the sodium aluminosilicates, Brooker *et al.*²⁹ found similar asymmetric peaks to Kohn *et al.*²⁸, again centered at ~163-165 ppm with a tail towards lower chemical shifts creating the asymmetry. They attributed these contributions to different species of “network carbonate” units, including Si-carbonate-Al and Al-carbonate-Al units. Brooker *et al.*²⁹ noted a weak peak at 171-175 ppm, suggesting that it may be related to a small amount of Na-carbonate ionic complexes present in their glasses. Recently Xue *et al.*³⁰ found results consistent with Brooker *et al.*²⁹ and expanded upon their findings.

Kim *et al.*³¹ recently used ¹³C MAS-NMR to study Na₂O·3SiO₂ glasses prepared under a range of pressures from 4 to 8 GPa, and found that the CO₃²⁻ free carbonate peak near 170 ppm shifted to lower frequency with increasing pressure, with the peak positions from 171.7 ppm at 4 GPa to 170.2 ppm at 8 GPa. Our corresponding Na₂O·3SiO₂ glass (*x* = 0.25) contained extremely low (0.003 wt%) carbon and consequently we were unable to obtain an NMR signal. However, due to being prepared under high pressure, Kim *et al.*'s³¹ glass contained 0.09 – 0.27 wt % ¹³CO₂ and thus they obtained a ¹³C MAS-NMR signal, albeit with a modest signal-to-noise ratio. The absence of any peaks at ~160-165 ppm in the spectra for all glasses studied here (Figure 3) also confirms the absence of bridging carbonates such as ^[4]Si(CO₃)^[4]Si or the network carbonate units described by Brooker *et al.*²⁹ and Xue *et al.*³⁰. Such units were also observed by Kim *et al.*³¹ in their Na₂O·3SiO₂ melts, but only at pressures of 6 GPa and above. Such network carbonate units are therefore not expected in sodium silicate glasses melted at ambient pressures, and the absence of peaks at ~160-165 in our ¹³C MAS-NMR spectra (Figure 3) confirms this. It can therefore be confidently demonstrated that essentially all carbon in all samples studied here is present in the form of ionic CO₃²⁻ units. As noted previously, we can conclude that these CO₃²⁻ units are surrounded by Na⁺ ions, forming nanoscale domains within the sodium silicate glass network.

For the first time, we have prepared and studied sodium silicate glasses across a very wide range of compositions, from (mol%, nominal) 20Na₂O·80SiO₂ to 70Na₂O·30SiO₂, in incremental steps of 5 mol%. This, and our other work on these glasses, soon to be published, augments and expands upon previous work including the highly-cited 1991 paper by Maekawa *et al.*⁴ The glass

formation region within the $\text{Na}_2\text{O-SiO}_2$ system that is readily accessible to standard melt-pour glassmaking approaches ends at 50-55 mol% Na_2O , as we have demonstrated here, and as also indicated by Maekawa *et al.*⁴, who quenched their melts in water or liquid N_2 . Only by extremely rapid quenching, accessed in this study by our novel roller-quench apparatus, has it been possible to access glasses with very high Na_2O contents of up to 70 mol%. In so doing, we have established new information on this archetypal yet simple glass-forming system. Crucially, we have shown that this “traditional” glass-formation boundary of approximately 50-55 mol% Na_2O also represents the point at which, from a structural and technological perspective, CO_2 retention as carbonate achieves significant levels (0.5 weight %) and then rapidly increases with further increases in nominal Na_2O content of the glass. This is also the nominal Na_2O content above which the carbonate anions are sufficiently abundant so as to have significant structural impacts on the glass, as evidenced by the changes we observe in the peak widths and positions in ^{23}Na MAS-NMR spectra (Figure 7).

Furthermore, neutron and X-ray diffraction experiments have been carried out, and will be reported in a future publication, which will describe the structural changes that take place over this wide range of compositions. It will also examine carbonate retention in terms of abundance, amorphous character, bond lengths, and bond angles. Further, the sodium-oxygen bond character will be presented. Also, a paper is in preparation detailing results from ^{29}Si MAS-NMR, Raman spectroscopy, thermal property analysis and density measurements. The three papers will present a thorough view of the various structural changes taking place in this most important glass system.

Our results therefore have implications for multiple fields of research. First, in carbonate glass-forming systems, geological melts, liquids and volatiles^{18-23,25,26} as our results provide important information on structural changes upon incorporation and retention of large amounts of carbonate in silicate melts and glasses prepared under atmospheric pressures, unlike previous studies conducted under pressure. In particular, we see evidence from both carbon and sodium MAS-NMR for glassy carbonate in at least two structural roles in the highest Na_2O -content glasses. Second, in glass science^{4,8-14} as our results extend the established range of the $\text{Na}_2\text{O-SiO}_2$ glass-forming system and show structural and compositional evolution as a result of carbonate incorporation. Third, in glass technology²⁴ as our results show that stable carbonate-rich glasses can be produced at the extreme ends of the simple glass-forming systems on which many technological glasses are based that retain only parts-per-million levels of CO_2 (e.g. commercial $\text{Na}_2\text{O-CaO-SiO}_2$ glass systems), implying opportunities for enhanced carbonate incorporation in technological glass-forming systems and potentially providing new glass properties and functionalities, also with potential for future carbon capture opportunities.

V. Conclusions

Sodium environments and carbonate retention in the widest-yet-studied compositional range of $\text{Na}_2\text{O-SiO}_2$ glasses were investigated using a range of complementary quantitative means. These included multinuclear nuclear magnetic resonance and carbon elemental assay. The results show CO_3^{2-} retention beginning with trace amounts at 40 mol% Na_2O (elemental analysis) and ^{13}C NMR detection at 40 mol% Na_2O . Based on our ^{23}Na MAS NMR results, Na-O bond lengths

decrease linearly with increasing Na₂O content of the glasses, up to 60 mol% Na₂O. Carbonate retention accelerates greatly with increasing Na₂O contents above 60 mol%. The carbonate anions are necessarily surrounded by Na⁺ ions, and are shown to be present in a form of dissolved, locally disordered, nanoscale domains. At 70 mol% Na₂O the weight fraction of carbonate in the glass exceeds 15%. Results from both ¹³C and ²³Na MAS-NMR are consistent with the 70 mol% Na₂O glass containing both short-range ordered sodium carbonate and amorphous sodium carbonate environments.

VI. Acknowledgements

M.P., M.A. and S.F. thank the US National Science Foundation for supporting this work under grant number NSF-DMR 1746230. M.C.W and P.A.B. acknowledge with thanks support from EPSRC under grant EP/R036225/1.

VII. References

1. F. Baino, Bioactive glasses – When glass science and technology meet regenerative medicine, *Ceramics International*, 2018, **44**, 14953-14966. <https://doi.org/10.1016/j.ceramint.2018.05.180>
2. E. Axinte, Glasses as engineering materials: A review, *Materials & Design*, 2011, **32**, 1717-1732. <https://doi.org/10.1016/j.matdes.2010.11.057>
3. S. Prasad, T. M. Clark, T. H. Sefzik, H.-T. Kwak, Z. Gan and P. J. Grandinetti, Solid-state multinuclear magnetic resonance investigation of Pyrex(R), *Journal of Non-Crystalline Solids*, 2006, **352**, 2834-2840. <https://doi.org/10.1016/j.jnoncrysol.2006.02.085> Doi:
4. H. Maekawa, T. Maekawa, K. Kawamura and T. Yokokawa, The structural groups of alkali silicate glasses determined from ²⁹Si MAS-NMR, *Journal of Non-Crystalline Solids*, 1991, **127**, 53-64. [https://doi.org/10.1016/0022-3093\(91\)90400-Z](https://doi.org/10.1016/0022-3093(91)90400-Z)
5. H. Zhang, S. Koritala, K. Farooqui, R. Boekenhauer, D. Bain, S. Kambeyanda, and S. Feller, A Model for Carbon Retention Dioxide Retention in Alkali Borate and Borosilicate Systems, *Physics and Chemistry of Glasses*, 1991, **32**(5), 185-187
6. J.Kasper, S. Feller, and G.Sumcad, New Sodium-Borate Glasses, *Journal of American Ceramic Society*, 1984, **67** No. 4 C-71
7. S.W. Martin and C.A. Angell, Glass formation and transition temperatures in sodium and lithium borate and aluminoborate melts up to 72 mol.% alkali, *Journal of Non-Crystalline Solids*, 1984, **66**, 429-442. [https://doi.org/10.1016/0022-3093\(84\)90368-5](https://doi.org/10.1016/0022-3093(84)90368-5)
8. M. G. Mortuza, R. Dupree and D. Holland, Studies of the effect of paramagnetic impurity in the structure of sodium disilicate glass, *Journal of Materials Science*, 2000, **35**, 2829-2832. <https://doi.org/10.1023/a:1004751303503>
9. X. Xue, M. Kanzaki, P. Floury, T. Tobase and J. Eguchi, Carbonate speciation in depolymerized and polymerized (alumino)silicate glasses: Constraints from ¹³C MAS and static NMR measurements and ab initio calculations, *Chemical Geology*, 2018, **479**, 151-165. <https://doi.org/10.1016/j.chemgeo.2018.01.005>
10. C. Dybowski, E. J. Gaffney, A. Sayir and M. J. Rabinowitz, Solid-state ¹³C and ²⁹Si MAS NMR spectroscopy of silicon carbide, *Colloids and Surfaces A: Physicochemical and Engineering Aspects*, 1996, **118**, 171-181. [https://doi.org/10.1016/0927-7757\(96\)03735-1](https://doi.org/10.1016/0927-7757(96)03735-1)

11. A. R. Jones, R. Winter, G. N. Greaves and I. H. Smith, ^{23}Na , ^{29}Si , and ^{13}C MAS NMR Investigation of Glass-Forming Reactions between Na_2CO_3 and SiO_2 , *The Journal of Physical Chemistry B*, 2005, **109**, 23154-23161. <https://doi.org/10.1021/jp053953y>
12. S. K. Lee and J. F. Stebbins, The distribution of sodium ions in aluminosilicate glasses: a high-field Na-23 MAS and 3Q MAS NMR study, *Geochimica Et Cosmochimica Acta*, 2003, **67**, 1699-1709. [https://doi.org/10.1016/s0016-7037\(03\)00026-7](https://doi.org/10.1016/s0016-7037(03)00026-7)
13. X. Xue and J. F. Stebbins, ^{23}Na NMR chemical shifts and local Na coordination environments in silicate crystals, melts and glasses, *Physics and Chemistry of Minerals*, 1993, **20**, 297-307. <https://doi.org/10.1007/bf00215100>
14. J. F. Stebbins, Cation sites in mixed-alkali oxide glasses: correlations of NMR chemical shift data with site size and bond distance, *Solid State Ionics*, 1998, **112**, 137-141. [https://doi.org/10.1016/s0167-2738\(98\)00224-0](https://doi.org/10.1016/s0167-2738(98)00224-0)
15. D. Massiot, F. Fayon, M. Capron, I. King, S. Le Calvé, B. Alonso, J. O. Durand, B. Bujoli, Z. Gan, G. Hoatson, 'Modelling one and two-dimensional solid-state NMR spectra.', *Magn. Reson. Chem.* 40 70-76 (2002) doi:10.1002/mrc.984
16. Z. E. M. Reeve, C. J. Franko, K. J. Harris, H. Yadegari, X. Sun and G. R. Goward, Detection of Electrochemical Reaction Products from the Sodium–Oxygen Cell with Solid-State ^{23}Na NMR Spectroscopy, *Journal of the American Chemical Society*, 2017, **139**, 595-598. <https://doi.org/10.1021/jacs.6b11333>
17. G. Chapuis, M. Dusek, M. Meyer and V. Petricek, Sodium carbonate revisited, *Acta Crystallographica Section B*, 2003, **59**, 337-352. <https://doi.org/10.1107/s0108768103009017>
18. M. Wilding, P. A. Bingham, M. Wilson, Y. Kono, J. W. E. Drewitt, R. A. Brooker and J. B. Parise, CO_{3+1} network formation in ultra-high pressure carbonate liquids, *Scientific Reports*, 2019, **9**, 15416.
19. M. Wilding, B. L. Phillips, M. Wilson, G. Sharma, A. Navrotsky, P. A. Bingham, R. Brooker and J. B. Parise, The structure and thermochemistry of $\text{K}_2\text{CO}_3 - \text{MgCO}_3$ glass, *Journal of Materials Research*, 2019, **34**, 3377-3388.
20. A. P. Jones, M. Genge and L. Carmody, Carbonate melts and carbonatites. In *Carbon in Earth*, R. M. Hazen, A. P. Jones, and J. A. Baross, eds., The Mineralogical Society of America, Chantilly, Virginia, 2013, pp. 289–322.
21. J. G. Blank and R. A. Brooker, Experimental studies of carbon dioxide in silicate melts: solubility, speciation and stable carbon isotope behaviour, in *Reviews in Mineralogy, Volatiles in Magmas*, M. R. Carroll and J. R. Holloway, eds., The Mineralogical Society of America, Washington D. C., 1994, 30, pp. 157-186.
22. J. R. Holloway and J. G. Blank, Application of experimental results to C-O-H species in natural melts, in *Reviews in Mineralogy, Volatiles in Magmas*, M. R. Carroll and J. R. Holloway, eds., The Mineralogical Society of America, Washington D. C., 1994, 30, pp. 187-230.
23. R. A. Lange, The effect of H_2O , CO_2 and F on the density and viscosity of silicate melts, in *Reviews in Mineralogy, Volatiles in Magmas*, M. R. Carroll and J. R. Holloway, eds., The Mineralogical Society of America, Washington D. C., 1994, 30, pp. 331-370.
24. F. T. Wallenberger and P. A. Bingham, Eds, *Fiberglass and glass technology: energy-friendly compositions and applications*, Springer, New York, 2010, 451 pages.

25. R. A. Brooker, S. C. Kohn, J. R. Holloway and P. F. McMillan, Structural controls on the solubility of CO₂ in silicate melts Part I: bulk solubility data, *Chemical Geology*, 2001, **174**, 225-239.
26. H. Ni and H. Keppler, Carbon in silicate melts, in Reviews in Mineralogy and Geochemistry, R. M. Hazen, A. P. Jones and J. A. Baross, eds., The Mineralogical Society of America, Washington D. C., 2013, 75, pp. 251-287.
27. A. R. Jones, R. Winter, P. Florian and D. Massiot, Tracing the Reactive Melting of Glass-Forming Silicate Batches by In Situ ²³Na NMR, *The Journal of Physical Chemistry B*, 2005, **109**, 4324-4332. <https://doi.org/10.1021/jp045705s>
28. S. C. Kohn, R. A. Brooker and R. Dupree, ¹³C MAS NMR: A method for studying CO₂ speciation in glasses, *Geochimica et Cosmochimica Acta*, 1991, **55**, 3879-3884.
29. R. A. Brooker, S. C. Kohn, J. R. Holloway, P. F. McMillan and M. R. Carroll, Solubility, speciation and dissolution mechanisms for CO₂ in melts on the NaAlO₂-SiO₂ join, *Geochimica et Cosmochimica Acta*, 1999, **63**, 3549-3565.
30. X. Xue, M. Kanzaki, P. Floury, T. Tobase and J. Eguchi, Carbonate speciation in depolymerized and polymerized (alumino)silicate glasses: Constraints from ¹³C MAS and static NMR measurements and ab initio calculations, *Chemical Geology*, 2018, **479**, 151-165.
31. E. J. Kim, Y. Fei and S. K. Lee, Effect of pressure on the short-range structure and speciation of carbon in alkali silicate and aluminosilicate glasses and melts at high pressure up to 8 GPa: ¹³C, ²⁷Al, ¹⁷O and ²⁹Si solid-state NMR study, *Geochimica et Cosmochimica Acta*, 2018, **224**, 327-343.